Fusion Engineering and Design 220 (2025) 115295

Contents lists available at ScienceDirect

Fusion Engineering and Design

journal homepage: www.elsevier.com/locate/fusengdes

Integrated design and analysis of optical performance for the ITER T-monitor high-power laser diagnostic

I. Ivashov [a,*], Yu. Krasikov [a], G. Sergienko [a], A. Huber [a], Ph. Mertens [b], M. Zlobinski [a], Ch. Linsmeier [a], Ph. Andrew [c], Jiang Xi [c]

[a] Institute of Fusion Energy and Nuclear Waste Management–Plasma Physics, Forschungszentrum Jülich GmbH, Germany
[b] FUSE-L Fusion Specific Expertise-Liege, Route du Condroz 111B, B-4031 Liège, Belgium
[c] ITER Organization, Route de Vinon, CS 90 046, 13067 Saint-Paul-lez-Durance, France

ARTICLE INFO

Keywords:
ITER diagnostics
Laser heating
Optical system
Ray-tracing

ABSTRACT

In order to measure the tritium content accumulated in the divertor tiles by residual gas analysis, ITER T-monitor diagnostic utilizes a powerful laser beam guided through a developed system of mirrors to heat locally a thin deposition layer on the divertor tiles Huber et al. [1]. The primary challenges identified include mirror surface distortion induced by laser heating, leading to potential issues such as loss of laser spot position and beam defocus. These concerns present a risk of desorption occurring at uncontrollable locations within the laser spots, thereby complicating the analysis. Due to the defocusing, not all of the tritium content in the heated area (typically within a 5 mm diameter spot) is desorbed, which could be compensated by increased laser power requiring a more complicated and expensive laser system.

The laser beam path consists of 15 mirrors in total. Six of them are located inside an equatorial port plug and, therefore, subjected not only to specific challenges associated with in-port components including thermo-mechanical loads, but also stringent integration requirements, and the necessity for remote handling capabilities.

This work presents the current design and analysis of the in-port optical components of the T-monitor diagnostic, focusing on its operation that starts after plasma operation (POS) and a six-hour cooldown period.

1. In-vessel system design overview

The in-vessel optical system consists of two main assemblies Front Mirror Box (FMB) and Rear Mirror Box (RMB), each containing three mirror units. The boxed are mounted on the Vertical Plates of the Diagnostic Shielding Module (DSM) (Fig. 1).

Each mirror box contains three mirror units mounted on a retractable Holder unit (Fig. 2). Holders are mounted to removable Housing units. Housing and Holder of FMB are cooled actively by water. Housing units are mounted on Brackets and permanently connected to the DSM. Mirrors are made of CuCrZr alloy with Au coating, most other structural parts are made of 316 L(N)-IG stainless steel.

2. Estimation of image quality distortion

An overview of the diagnostic system's optical layout can be found in [1]. Two main optical performance criteria are set for the T-monitor diagnostic:

1. A safety requirement: beam spot shift from nominal position < 1mm – to prevent from heating the divertor cooling pipes
2. Measurement accuracy requirement: ensure that the uncertainty of the desorbed surface area does not exceed 10 %. Assuming a near flat-top power distribution, the uncertainty can be approximated as:

$$\Delta A \Big/ A \approx \frac{P\delta}{A} \rightarrow \delta \approx (\Delta A / A)\frac{A}{P}$$

where $\Delta A/A$ is the desorbed surface area uncertainty, A – nominal surface area, P – perimeter, δ - required spot radius tolerance.

For a single spot operation mode this tolerance is around 128 μm (5 mm diameter circle), for one divertor tile – 430 μm (31 mm x 12 mm rectangle). The final tolerance requirements are defined as the square root sum of squares of the spot radius tolerance and the diffraction limit (125 μm), yielding 180 μm for a single spot operation mode, and 450 μm

* Corresponding author.
E-mail address: i.ivashov@fz-juelich.de (I. Ivashov).

https://doi.org/10.1016/j.fusengdes.2025.115295
Received 17 January 2025; Received in revised form 26 May 2025; Accepted 19 June 2025
Available online 9 July 2025

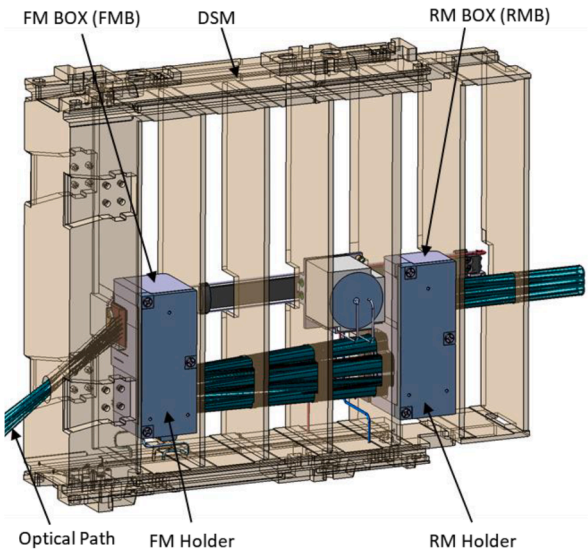

Fig. 1. FMB and RMB arrangement inside DSM.

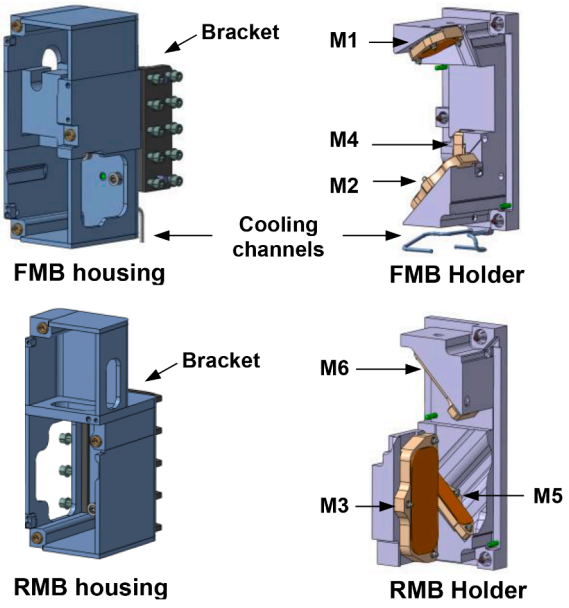

Fig. 2. Exploded views of FMB and RMB.

for operation modes covering one or more tiles with a series of 5 mm pulses.

To verify the system's optical performance, a thermal-structural analysis is first performed in ANSYS. The resulting distorted mirror surfaces are then converted to Grid Sag surface files and exported to Zemax for ray-tracing analysis.

2.1. Thermo-mechanical modeling

Tritium monitor operation starts 6 h after a series of ITER plasma operation cycles. For thermal analysis of FMB and RMB the following load steps were taken into account:

1. Baking sequence – 34 h coolant temperature ramp up to 240 °C, 14 h flat top, 24 h coolant temperature ramp down to 70 °C. Since the RMB is not actively cooled and the plasma operation sequence may begin immediately after Baking, this analysis step is required to estimate the resulting temperature of the RMB;

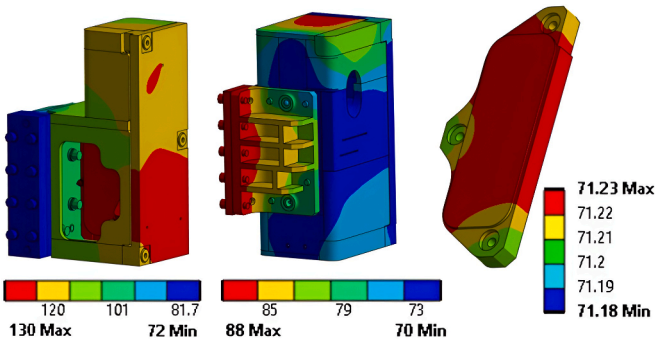

Fig. 3. Temperature distribution (°C) after 6h cooldown (from left to right): Rear Mirror box, Front Mirror box, M4.

2. Plasma operation sequence – 20 plasma cycles, 450s burn (neutronic load), 1350 s dwell time, 10 h total;
3. Cooldown phase after plasma operation – 6h;
4. Tritium monitor operation – surface heating of the mirror surfaces by laser beam.

The boundary conditions include temperatures at the mounting interfaces, ambient temperature values for radiation heat transfer and water convective cooling for the FMB water loop. The temperature distribution for the FMB, RMB and M4 after 6 h cooldown are shown in Fig. 3.

For the modeling of the laser operation sequence the most demanding planned scenario was taken: 192 pulses over 3 s with a pulse duration of 3 ms and 12.625 ms interval between pulses; total laser power is 25.5 kW (1070 nm). In this scenario eight tiles are heated in poloidal direction; the sequence of laser pulses is shown in Fig. 4.

Each mirror surface is subjected to a corresponding elliptical surface heat load with Gaussian power distribution. The center of the spot moves along the mirror surface in a zig-zag pattern shown in Fig. 4. The total absorbed power per pulse ranges from 570W (M1) to 703W (M6), which corresponds to the surface reflectivity of 96 % (based on the measurements of a similar diagnostic setup at JET [2]). The resulted temperature distribution for M4 (highest power density) at the end of 192nd pulse is shown in Fig. 5.

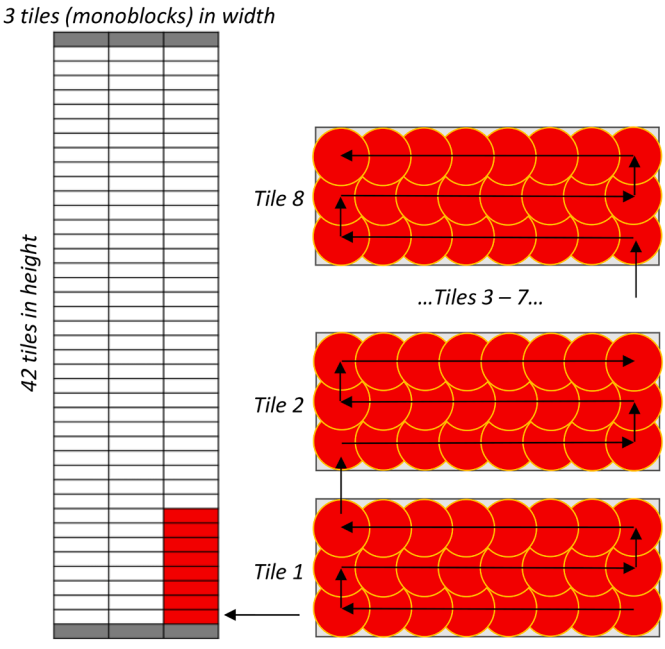

Fig. 4. The T-monitor diagnostic FOV and eight tiles divertor scanning scheme.

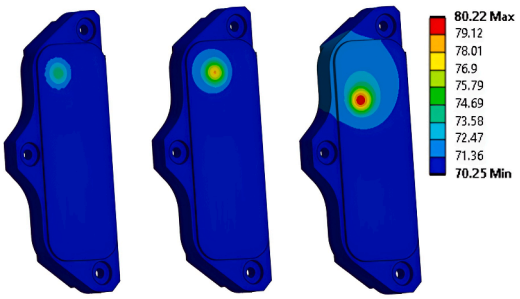

Fig. 5. Temperature distribution (°C) at the end of 1st, 24th and 192nd pulses for M4 (from left to right).

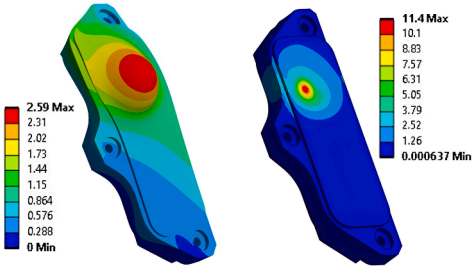

Fig. 6. Total deformation (μm, left) and Von-Mises stress (MPa, right) of M4 after 192nd pulse (only laser load).

For the structural analysis of FMB and RMB, assuming a quasi-static approximation, the following steps were taken into account:

1. System assembly (bolt preload and dead weight)
2. Non-uniform temperature field after plasma operation (neutron heating) and 6 h dwell
3. Non-uniform temperature field after each of the 192 laser pulses (8 tiles scan)

In addition, only the laser loads without the assembly loads and thermal loads after POS were simulated for all the laser pulses as a case of ideal mirror mounting. The shifts and rotations of the mounting interfaces due to the DSM deformation are not considered in the current work and will be assessed later. The deformed M4 shape for this idealized scenario is shown in Fig. 6.

2.2. Ray-tracing analysis

The ray-tracing analysis was conducted in Zemax using the distorted mirror surfaces for each case (1, 2, 3, 3*, 4, 4*) for the scanning mirror position corresponding to the location of the 1st pulse (also representing a single pulse mode) and 192nd pulse for the wavelengths of 1070 nm (blue, main laser), 685 nm (green, pilot laser) and 650 nm (red, pilot laser). The overview of the main analysis results is presented in Table 1.

The results show that the system assembly load (case #1) does not significantly affect the image quality compared to the nominal case (case #0). Minor spot position shift can be corrected by re-adjustment during the assembly.

Since the T-monitor diagnostic will operate at elevated temperature, the displacement results are corrected by subtracting the corresponding loadstep with homogenous heating of FMB and RMB to 70 °C (coolant temperature) for the cases #2 and #3.

Right before the Tritium monitor operation (case #2), the curvature of the toroidal mirror M3 increases due to the elevated temperature (see Fig. 3, RMB; M3 is directly facing the cutout) the image becomes defocused. Refocusing at this step is possible which reduces the spot RMS radius to ~75 μm, within the upper limit of 180 μm for the single pulse mode. The temperature expansion of the components causes a shift in the beam center from its nominal position, by -2.28/-2.32 mm in the toroidal direction and +1.85/+1.69 mm in the poloidal direction for 1st and 192nd pulses respectively. This shift is addressed by repositioning every laser spot within the available field of view using a pilot laser.

The RMS radius 100 μm for the single pulse scenario (case #3, left) is well within the limit of 180 μm) and the spot position shift is negligible considering the abovementioned target area repositioning. After the 192nd laser pulse (case #3, right) the image is significantly distorted with spot RMS radius of 1427 μm. In case of the active refocusing during the scan (case #3*, right), the spot RMS radius can be reduced to 370 μm which complies with the limit of 450 μm, but the poloidal shift of around 1.5 mm (considering prior repositioning of 1.69 mm for case #2 minus 0.2 mm for case #3*) violates the safety limit of 1 mm.

Cases #4 and #4* represent a laser operation scenario with an ideal mounting to exclude the influence of the bolt preload and pre-operation temperature. Respective comparison to cases #3 and #3* shows very little influence of the mounting and initial temperature.

It should be noted that current analysis takes into account only the influence of the in- vessel mirrors deformation, assuming the deformation of the ex-vessel mirrors negligible due to the usage of Zerodur [1], which will be further investigated during the next design stage.

3. Discussion

The results show that it is unlikely to meet the criteria for the 3 ms 8-tile scanning scenario unless a coating with significantly higher reflectivity is adopted. Extensive testing is required to identify a viable solution that maintains its performance during the Tritium monitor lifetime.

Active refocusing can be implemented by preprogramming specific focusing mirror positions based on simulation results. Cases #3 and #4 with active refocusing represent the most optimistic scenario, assuming both the simulation is perfectly accurate and the focusing mirror can precisely track the pre-programmed positions in real time, which may not be achievable in practice.

Another option is to reduce the pulse duration, which requires higher total power to keep the same surface temperature (for large spot size $T_{max} \sim q\sqrt{t}\ \left[J/\sqrt{s}\ \ /m^2\right]$ [3]), but reduces the deformation of the mirror surface (for large spot size $u_z \sim qt\ \left[J/m^2\right]$, can be shown using methods from [4]). The same analysis sequence was conducted for another foreseen scenario: 192 pulses over 3 s with a pulse duration of 1 ms and total power of 44 kW [1]. The spot RMS radius for the last pulse of the sequence for cases #3, #3* and #4, #4* are around 840 nm and 230 nm respectively, which is in line with the theory: approximately $\sqrt{3}$ smaller compared to the 3 ms scenario.

4. Summary

Ray-tracing analysis of optical components is essential for validating the performance of the high-power laser system and for defining its acceptable operational parameters. To verify the optical performance, a thermal-mechanical simulation was first conducted in ANSYS, taking into account the system assembly, plasma operation, post-plasma operation, and the Tritium monitor laser scanning procedure. The resulting distorted mirror surfaces were then exported to Zemax for ray-tracing analysis.

The main optical performance parameters defined are RMS radius (loss of sharpness) and spot shift (FOV limits, possible divertor cooling pipe targeting). Current design of the in-port optical system satisfies the optical criteria on spot defocusing and position shift for a single spot scenario. For the 3 ms 8-tile scanning scenario, the thermal deformations of the mirror surfaces are too significant to meet the required limits, but corrective measures like dynamic refocusing and repositioning (with larger margins to the edges) as well as shorter higher power pulses are under consideration. Different mirror coatings will also be tested to

Table 1
Raytracing analysis results for the points corresponding to the location of the 1st and 192nd pulse.

Case #	Load case Description	1st Pulse				192nd Pulse			
		Spot diagram	RMS Radius, Centroid [μm]	Spot position shift on divertor [mm]		Spot diagram	RMS Radius, Centroid [μm]	Spot position shift on divertor [mm]	
				Toroidal	Poloidal			Toroidal	Poloidal
0	Nominal mirror surfaces (nominal focus)	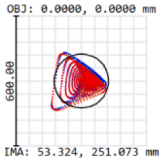	79	0.00	0.00	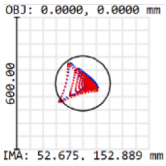	55	0.00	0.00
1	Bolt preload and dead weight at RT (nominal focus)	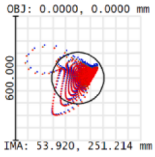	83	-0.60	-0.14	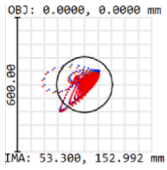	56	-0.63	-0.10
2	6 h after plasma operation (geometry adjusted to 70° C, refocused)	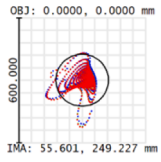	72	-2.28	1.85	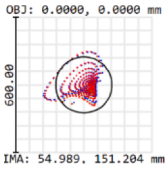	74	-2.32	1.69
3	Laser load (geometry adjusted to 70° C, case #2 focus)	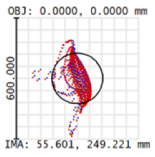	100	-2.28	1.85	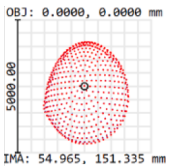	1427	-2.29	1.55
3*	Laser load (geometry adjusted to 70° C, active refocusing)	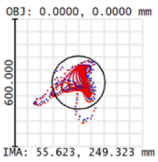	74	-2.30	1.75	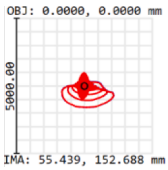	370	-2.76	0.20
4	Laser load only (nominal focus)	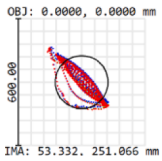	104	-0.01	0.01	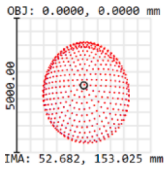	1439	-0.01	-0.14
4*	Laser load only (active refocusing)	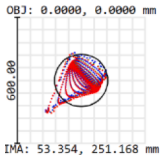	83	-0.03	-0.09	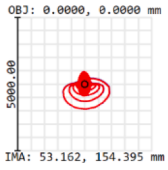	354	-0.49	-1.51

determine if an option with a reflectivity greater than 96 % can be maintained throughout the diagnostic lifetime.

CRediT authorship contribution statement

I. Ivashov: Writing – review & editing, Writing – original draft, Visualization, Validation, Software, Methodology, Investigation, Formal analysis, Conceptualization. **Yu. Krasikov:** Writing – review & editing, Writing – original draft, Supervision, Project administration, Methodology, Data curation, Conceptualization. **G. Sergienko:** Supervision, Methodology, Investigation, Formal analysis, Data curation, Conceptualization. **A. Huber:** Supervision, Project administration, Funding acquisition, Conceptualization. **Ph. Mertens:** Writing – review & editing, Supervision. **M. Zlobinski:** Methodology, Conceptualization. **Ch. Linsmeier:** Writing – review & editing, Project administration, Funding acquisition. **Ph. Andrew:** Project administration. **Jiang Xi:** Project administration.

Declaration of competing interest

The authors declare that they have no known competing financial interests or personal relationships that could have appeared to influence the work reported in this paper.

Acknowledgments

We would like to express our gratitude to our colleagues, D. van Staden, S. Eberle, D. Kampf and A. Reutlinger from KTO for their support and collaboration throughout this project.

This work is supported by the ITER Organization within the framework of the Cooperation Agreement on Academic, Scientific, and Technical Cooperation between Forschungszentrum Jülich GmbH and the ITER International Fusion Energy Organization (ITER ref. IO/21/CT/4300002506). The views and opinions expressed herein do not necessarily reflect those of the ITER Organization.

Data availability

The authors do not have permission to share data.

References

[1] A. Huber, et al., A laser-based diagnostic for in situ monitoring of fuel retention in ITER, Fusion Eng. Design 219 (2025) 115298.
[2] M. Zlobinski, et al., First results of laser-induced desorption-quadrupole mass spectrometry (LID-QMS) at JET, Nucl. Fusion 64.8 (2024) 086031.
[3] H.S. Carslaw, J.C. Jaeger, Conduction of Heat in Solids, 2nd ed., Clarendon Press, 1959.
[4] H. Parkus, Instationäre Wärmespannungen, Springer-Verlag, 1959.